Sugar-Derived Cyclic Acetals as Comonomers for Cationic Copolymerization with Vinyl Ethers

*Aya Katto, Sadahito Aoshima, and Arihiro Kanazawa**

Department of Macromolecular Science, Graduate School of Science, Osaka University, Toyonaka, Osaka 560-0043, Japan

For TOC Use Only:

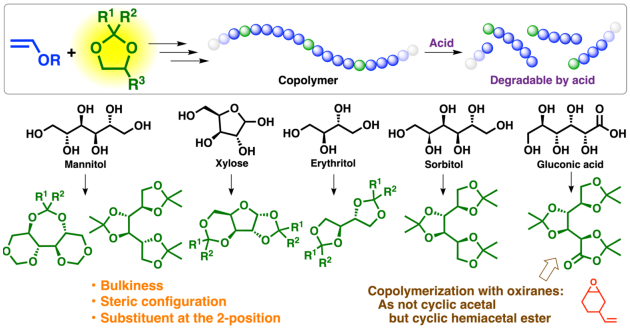

Abstract

Sugar-derived cyclic acetals were demonstrated to undergo cationic copolymerization with a vinyl ether (VE) via the vinyl-addition and ring-opening mechanisms. Cyclic acetals were synthesized by the condensation reactions of sugar alcohols (mannitol, xylose, erythritol, and sorbitol) with aldehydes or ketones. These cyclic acetals differ in the number of cyclic acetal moieties, the number of ring members, substituents, and stereo configuration. Such structural features greatly affected the copolymerization behavior. For example, erythritol-derived cyclic acetals consisting of two isolated five-membered cyclic acetal moieties undergo copolymerization with 2-chloroethyl VE, while mannitol-derived cyclic acetals consisting of three fused seven- and six-membered cyclic acetal moieties were not incorporated into polymer chains. Moreover, a xylose-derived cyclic acetal that has a *p*-methoxyphenyl substituent at the carbon atom adjacent to two oxygen atoms underwent copolymerization most effectively among the cyclic acetals examined in this study, which is likely due to the efficient generation of a carbocation via ring-opening. In addition, cationic initiators or Lewis acid catalysts affected the frequency of crossover reactions, resulting in a difference in incorporated ratios of sugar-derived cyclic

acetals in polymer chains. The copolymers synthesized from VEs and sugar-derived cyclic acetals were degraded by acid via cleavage of the VE-to-cyclic acetal crossover reaction-derived acetal moieties in the main chain. A gluconic acid-derived cyclic acetal that has both cyclic acetal and cyclic hemiacetal ester moieties was ineffective for copolymerization with a VE, whereas an oxirane was successfully copolymerized with the gluconic acid-derived monomer via the ring-opening of the cyclic hemiacetal ester moiety.

Introduction

Various synthetic polymers are produced from petrochemicals for general purposes in our daily life all over the world, while there have been emerging problems of synthetic polymer (plastic) wastes that are unsuitably released into nature. Essential ways to solve the problem are to reduce the produced and used amounts of synthetic polymers and to recycle polymer wastes. Another strategy is to produce polymers from renewable feedstocks as alternatives for petrochemicals. Plant-derived compounds are promising as substrates for polymer synthesis. For example, polylactide,[1–3] which is derived from starch, has attracted attention as a sustainable polymer material for packaging.

Sugars are very attractive building blocks for polymer synthesis. A representative method of polymer synthesis from sugars is polycondensation of sugars and bifunctional monomers.[4–6] The hydroxy groups of sugars are directly used in bond-forming reactions, such as reactions with carboxy, acyl, or amino groups, in some studies, while reactive groups converted from the hydroxy groups are used in other studies. Sugars can also be transformed into monomers for chain-growth polymerization. For example, D-xylose-derived cyclic monomers having an oxetane ring were reported to yield high-MW polymers by ring-opening (co)polymerization.[7–13] An isosorbide-derived cyclic ether was also polymerized by the ring-opening mechanism.[14,15] In addition, anhydrosugars (Scheme 1B), which are synthesized by dehydration reactions of sugars, undergo cationic ring-opening polymerization (ROP) via single ring-opening of the bicyclic acetal structures[16–18] in a manner similar to cationic ROPs of not-

sugar-derived monocyclic and bicyclic acetals.[16,19,20] Recent examples of anhydrosugar polymerization include the design of new monomers and the living cationic polymerization of anhydrosugars.[21–23]

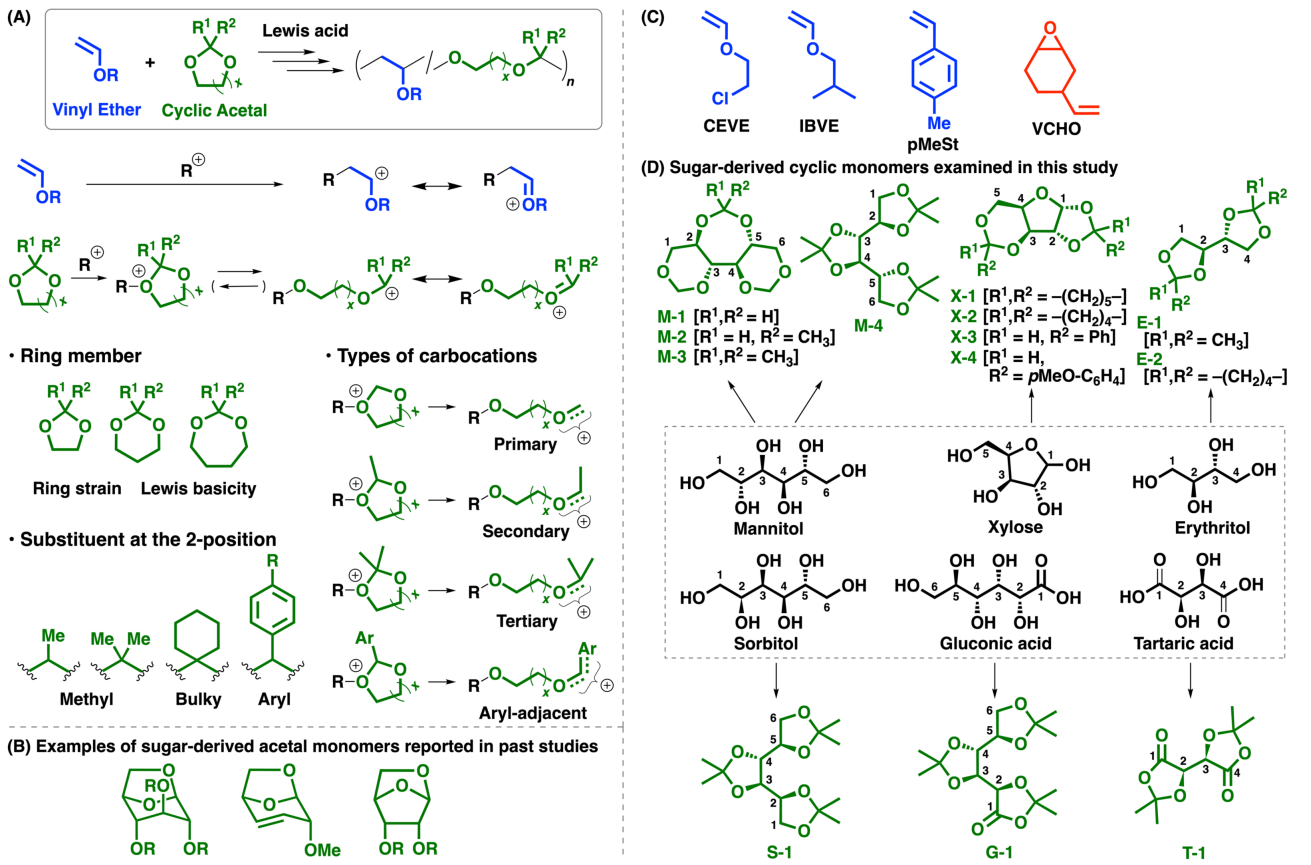

Scheme 1. (A) Cationic Copolymerizations of VEs and Cyclic Acetals. (B) Examples of Sugar-Derived Acetal Monomers in Previous Studies. (C) Vinyl Monomers and Oxirane Used in This Study. (D) Sugar-Derived Cyclic Monomers Examined in This Study.

Motivated by promising possibilities of sugars for polymer synthesis, we focused on sugar-derived cyclic acetals as monomers for ROP. Since early 1900s, various cyclic acetals were synthesized by condensation reactions of sugars and carbonyl compounds such as aldehydes and ketones.[24–39] Some sugar-derived cyclic acetals bearing hydroxy groups were used as monomers in polycondensation, yielding polymers with rigid cyclic structures in the main chains.[4] However, as far as we know, there have been no example that demonstrate ROP of sugar-derived cyclic acetals except for anhydrosugars. Cyclic acetals synthesized from various diols and carbonyl compounds were reported to undergo cationic copolymerization with vinyl monomers such as vinyl ethers (VEs) and styrene derivatives.[40,41] Carbocations adjacent to an oxygen atom (oxocarbenium ions) are generated from both VEs and cyclic

acetals (Scheme 1A). Our group has also developed the cationic copolymerizations of VEs and cyclic acetals with a focus on the effects of cyclic acetal structures on copolymerization (Scheme 1A).[42–44] The polymerizability of cyclic acetals depended on the number of ring members and the substituents. In particular, most of 2,2-dimethyl or 2-aryl cyclic acetals did not undergo homopolymerization but exhibited copolymerizability; hence, alternating copolymers were obtained by the copolymerizations with suitable VEs. Structural variation of sugar-derived cyclic acetals is a very attractive feature, considering the possibilities of cyclic acetals as comonomers for precision polymer synthesis by cationic copolymerization.

In this study, we investigated copolymerizations of VEs and sugar-derived cyclic acetals synthesized by condensations reactions of carbonyl compounds with sugar, sugar alcohols, aldonic acid, or aldaric acid, such as mannitol, xylose, erythritol, sorbitol, gluconic acid, and tartaric acid (Scheme 1D).[24–39] The synthesized monomers have two or three cyclic acetal moieties of five-, six-, or seven-membered rings in an independent or fused manner. As a result of systematic investigation on cationic polymerizations with 2-chloroethyl VE (CEVE; Scheme 1C), polymerizabilities of the cyclic acetals were demonstrated to differ depending on bulkiness, stereo configuration, and substituents. In addition, a monomer containing both cyclic acetal and cyclic hemiacetal ester moieties was found to undergo cationic copolymerization with oxiranes via the ring-opening of the latter moiety.

Experimental Section

See the Supporting Information.

Results and Discussion

Synthesis of Sugar-Derived Cyclic Acetals

Most of the sugar-derived cyclic acetals used in this study (M-1, M-4, X-1, X-2, X-3, X-4, E-1, E-2, S-1, G-1, and T-1 in Scheme 1D) were synthesized by one-step reactions from sugar, sugar alcohols,

aldonic acid, or aldaric acid according to the literature methods[24,25,28–39] (see the Experimental section in the Supporting Information). The one-step synthesis of the monomers is an advantage of this study. M-2 and M-3 (Scheme 1D) were synthesized by two-step reactions consisting of 1,3:4,6-di-*O*-methylene-D-mannnitol synthesis from D-mannitol and subsequent condensation with carbonyl compounds.[26,27]

Homopolymerization of Sugar-Derived Cyclic Acetals

Cationic homopolymerization of M-4, S-1, G-1, E-1, E-2, or X-4 was conducted using $SnCl_4$ or $Ph_3CB(C_6F_5)_4$ as a Lewis acid catalyst or a cationic initiator, respectively, in dichloromethane at −78 °C (Table S1). However, homopolymerizations of these monomers did not proceed at all. The results are consistent with our previous studies, which demonstrated nonhomopolymerizability of cyclic acetals with two substituents at the 2-position.[43,44] In the case of X-4, which consists of a diastereomeric mixture, the ratio of diastereomers changed after the reaction with $SnCl_4$ (from 89/11 to 71/29). This was likely because the cyclic acetal moiety in X-4 opened in the reaction with an acid, whereas the ring closed again without undergoing homopolymerization.

Cationic Copolymerization of CEVE and Sugar-Derived Cyclic Acetals

In our previous studies, CEVE, which is a low reactive VE due to the electron-withdrawing chlorine atom, was reported to undergo cationic copolymerizations with various cyclic acetals via crossover reactions. In this study, therefore, copolymerizations of CEVE and various sugar-derived cyclic acetals (Scheme 1D) were investigated with an initiating system consisting of IBVE–HCl (or IBVE-AcOH and $TiCl_4$, which generate IBVE–HCl in situ), $SnCl_4$, and ethyl acetate. This initiating system is effective for the controlled/living cationic copolymerization of CEVE and various cyclic acetals. The results are summarized in Table 1. M-1, M-2, and M-3,[24–27] which were obtained from D-(–)-mannitol and have seven- and six-membered cyclic acetal moieties, were not incorporated into polymer chains at all, while CEVE homopolymers were obtained (entries 1–3; see Figure S1 for the ^{1}H NMR

spectra). M-4 and S-1,[37–39] which were obtained from D-(–)-mannitol and D-(–)-glucitol, respectively, and have three five-membered rings, were incorporated into polymer chains (entries 4 and 5; see Figures S2 and S3 for the MWD curves and the ^{1}H NMR spectra, respectively), whereas G-1,[35,36] which was derived from D-(+)-glucono-1,5-lactone and has two five-membered cyclic acetals and one five-membered cyclic hemiacetal ester, was not incorporated into polymer chains (entry 6; Figures S2 and S3). Detailed comparisons of the M-4, S-1, and G-1 results are discussed later. E-1 and E-2,[31–34] which were obtained from *meso*-erythritol and have two five-membered rings, underwent copolymerizations with CEVE to yield copolymers with unimodal MWDs (entries 7 and 8; Figure 1; see Figure S4 for the ^{1}H NMR spectrum of the product from E-2).[45] In the cases of X-1, X-2, X-3, and X-4,[28–30] which were derived from D-(+)-xylose and have five- and six-membered cyclic acetal moieties, the substituents at the carbons adjacent to two oxygen atoms were responsible for the copolymerizations. X-1 and X-2, which have alkyl substituents, were not incorporated into polymer chains (entries 9 and 10; Figure S5), while X-3 and X-4, which have aromatic rings, underwent copolymerizations with CEVE (entries 11 and 12; Figure S6). In particular, X-4 was copolymerized with CEVE most effectively among the sugar-derived cyclic acetals examined in this study. The details are discussed later.

Table 1. Cationic Copolymerization of Various Sugar-Derived Cyclic Acetals with CEVE [a]

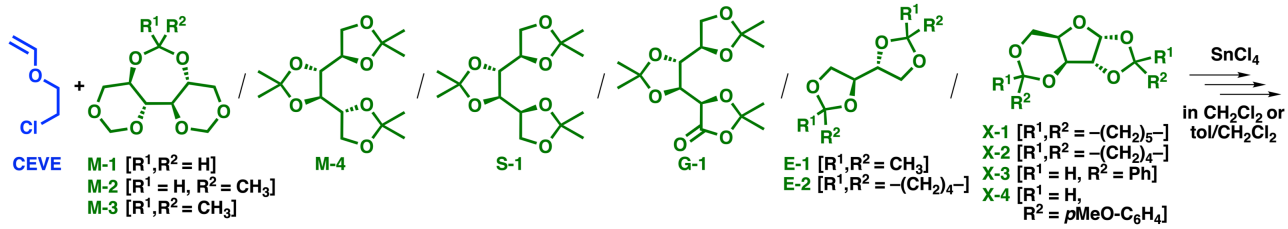

entry	conc (M)		temp (°C)	time	conv (%)		$M_n \times 10^{-3}$ (calcd)[d]	$M_n \times 10^{-3}$ (exp)[e]	M_w/M_n[e]	units per block[f]	
	CEVE	cyclic acetal			CEVE[b]	cyclic acetal[c]				CEVE	cyclic acetal
1	0.40	M-1 0.10	–6	3 min	>99	0	10.8	2.5	1.44	–	–
2	0.080	M-2 0.080	–40	1 min	98	0	10.6	2.2	1.49	–	–
3	0.40	M-3 0.40	–78	3 min	>99	0	10.8	7.7	1.07	–	–
4	0.40	M-4 0.40	–78	12 min	66	3	8.1	7.0	1.09	22	1.0
5	0.40	S-1 0.40	–78	15 min	87	2	10.0	7.3	1.06	51	1.0
6	0.40	G-1 0.40	–78	30 min	>99	0	10.8	7.0	1.08	–	–

7	0.40	E-1 0.40	–78	8 min	81	5	9.8	8.1	1.08	18	1.0
8	0.40	E-2 0.40	–78	15 min	74	4	9.0	5.8	1.12	17	1.0
9	0.40	X-1 0.40	–78	3 min	98	0	10.6	9.0	1.12	–	–
10	0.40	X-2 0.40	–78	1 min	92	0	9.9	8.5	1.13	–	–
11	0.40	X-3 0.40	–78	5 min	75	<1	8.1	4.2	1.12	(165)	1.0
12	0.40	X-4 0.40	–78	2 h	81	15	14.5	5.7	1.31	5.4	1.0

[a] Entries 1—8, 11, and 12: $[IBVE–HCl]_0$ = 1.0 (entry 2) or 4.0 mM (except for entry 2), $[SnCl_4]_0$ = 5.0 (entry 2) or 20 mM (except for entry 2), [ethyl acetate] = 13 (entry 2) or 50 mM (except for entry 2), in dichloromethane. Entries 9 and 10: $[IBVE–AcOH]_0$ = 4.0 mM, $[SnCl_4]_0$ = 20 mM, $[TiCl_4]_0$ = 5.0 mM, [ethyl acetate] = 20 mM, [2,6-di-*tert*-butylpyridine]$_0$ = 10 mM, in toluene/dichloromethane (9/1 v/v). [b] Determined by gas chromatography. [c] Determined by method B (see the experimental section for method B). [d] Calculated from the amounts of the cationogen and the consumed monomers: ($[CEVE]_0$ × conv × MW + [cyclic acetal]$_0$ × conv × MW)/$[IBVE–HCl]_0$. ($[CEVE]_0$ + [cyclic acetal]$_0$)/$[IBVE–HCl]_0$ = 200 (except for entries 1 and 2), 125 (entry 1), or 160 (entry 2). [e] Determined by GPC (polystyrene standards). [f] Estimated by ^{1}H NMR analysis. After purification by preparative GPC.

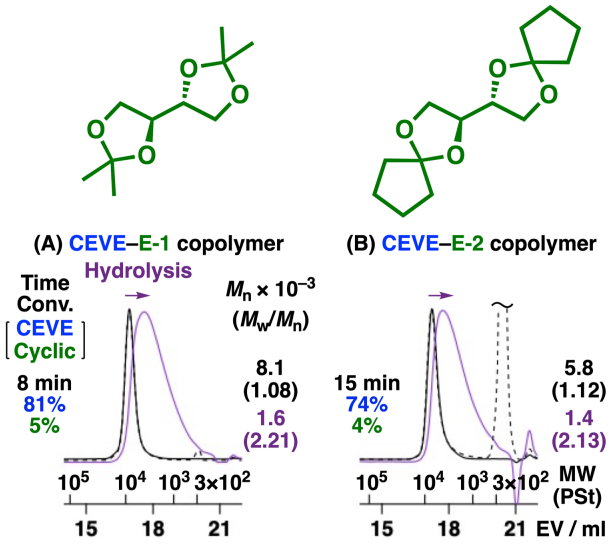

Figure 1. MWD curves of the (A) CEVE–E-1 (entry 7 in Table 1) and (B) CEVE–E-2 (entry 8) copolymers [black; before (dashed) and after (solid) purification by preparative GPC] and their hydrolysis products (purple; hydrolyzed after purification by preparative GPC). See Table 1 for the polymerization conditions.

The result of the copolymerization of CEVE and E-1 is explained in detail as a representative example. The copolymerization smoothly proceeded to reach CEVE conversion of 88% in 13 min (Figure 2A). The MWDs of the copolymers were very narrow and shifted to the higher-MW regions as the polymerization proceeded (Figure 2C), which indicates the generation of long-lived species. The M_n values of the copolymers linearly increased with an increase in monomer conversion (Figure 2B) although the values were lower than the theoretical values. Unintended initiation reactions from

adventitious water and the cyclic acetal–$SnCl_4$ interaction[44] are likely responsible for the results. These results suggest that the copolymerization proceeded in a living manner. Similar results were also obtained when E-2 and M-4 were used as cyclic acetals (Figures S7 and S8). Higher-molecular-weight polymers were obtained by the copolymerization at higher monomers/cationogen concentration ratios (Table S2).

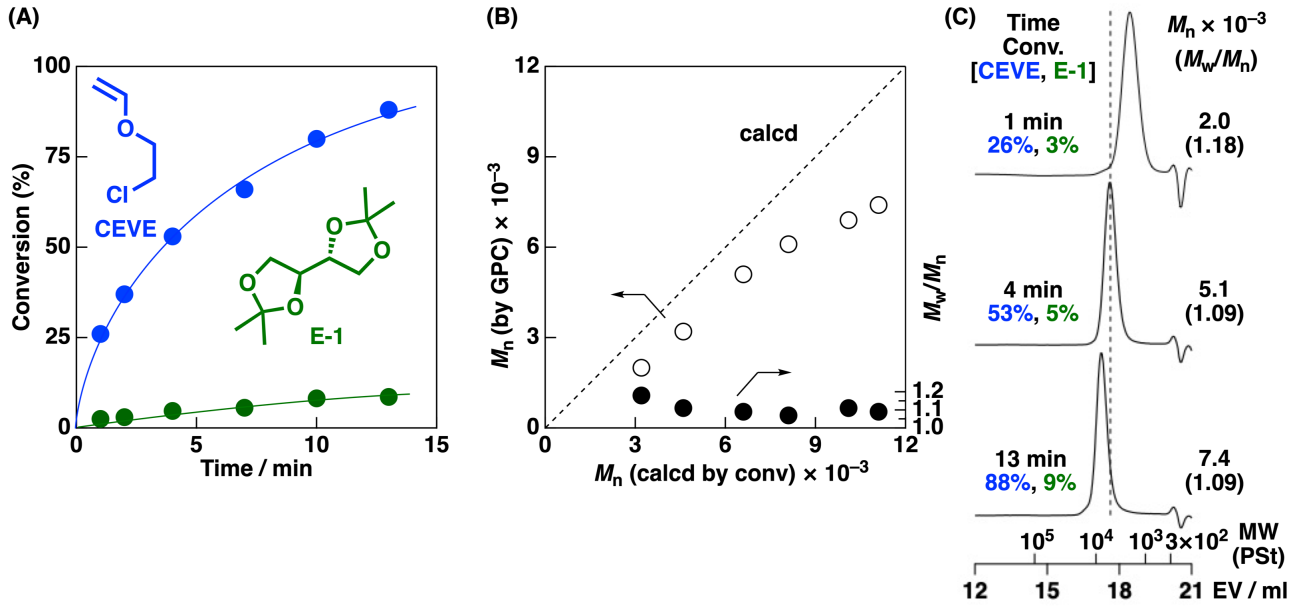

Figure 2. (A) Time–conversion curves for the copolymerization of CEVE and E-1, (B) the M_n (open circle) and M_w/M_n (filled circle) values of poly(CEVE-*co*-E-1)s, and (C) MWD curves of poly(CEVE-*co*-E-1)s. Polymerization conditions: $[CEVE]_0$ = 0.40 M, $[E\text{-}1]_0$ = 0.40 M, $[IBVE–HCl]_0$ = 4.0 mM, $[SnCl_4]_0$ = 20 mM, [ethyl acetate] = 50 mM, in dichloromethane at −78 °C. Conversion was determined by method A (see the experimental section for method A).

^{1}H NMR analysis of the copolymer obtained from CEVE and E-1 suggested that the copolymers were generated by the reactions between CEVE and E-1 (Figure 3A). Peaks at 1.5–2.0 ppm (peaks 1 and 12) were assignable to the methylene group of CEVE units in the main chain, while peaks at 1.2–1.4 ppm (8 and 11) were assigned to the methyl group of E-1 units. The peaks at 4.6–5.0 ppm (peak 5) were assigned to the acetal moieties derived from the crossover reaction from CEVE to E-1. The copolymer structures were also confirmed by ^{13}C and 2D (^{1}H–^{1}H COSY, ^{1}H–^{13}C HSQC, and ^{1}H–^{13}C HMBC) NMR analyses (Figures S9–S12). The average number of CEVE and E-1 units per block was calculated to be 18 and 1.0, respectively, from the integral ratios. The result of matrix-assisted laser desorption/ionization time-of-flight mass spectrometry (MALDI-TOF-MS) analysis (Figure S13) was also consistent with the

above results. Peaks with *m*/*z* values that correspond to polymer structures consisting of the cationogen-derived α-end, CEVE units, E-1 units, and the quencher-derived ω-end.

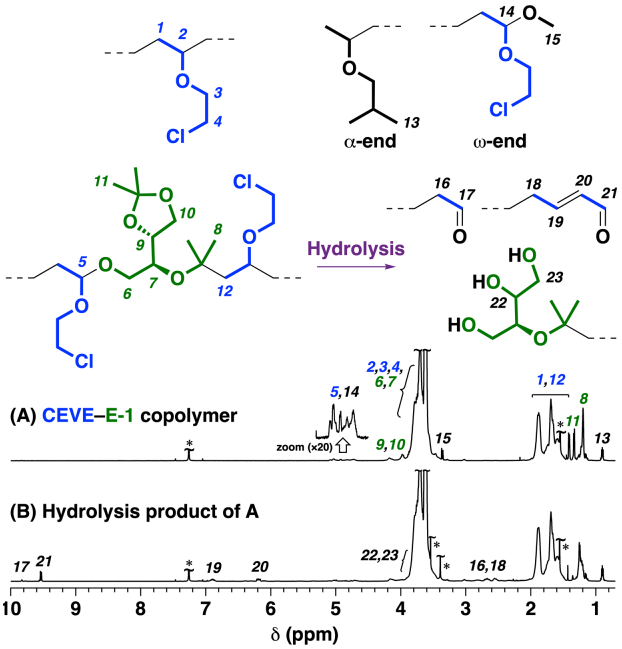

Figure 3. ^{1}H NMR spectra of (A) the CEVE–E-1 copolymer (entry 7 in Table 1; Figure 1A; after purification by preparative GPC) and (B) its hydrolysis product (purple curve in Figure 1A). * Water, $CHCl_3$, or 1,2-dimethoxyethane.

The obtained copolymer was subjected to acid hydrolysis, resulting in the cleavage of the acetal moieties in the main chain (Scheme 2). The ^{1}H NMR spectrum of the acid hydrolysis product (Figure 3B) did not exhibit the peaks of the acetal structures, which was observed in the original copolymer (peak 5), while aldehyde peaks were observed at 9.5 and 9.8 ppm (peaks 17 and 21). Moreover, the hydrolysis product had a lower M_n value than the original copolymer, which supports the cleavage of the acetals in the main chain (Figure 1A, purple; Scheme 2).

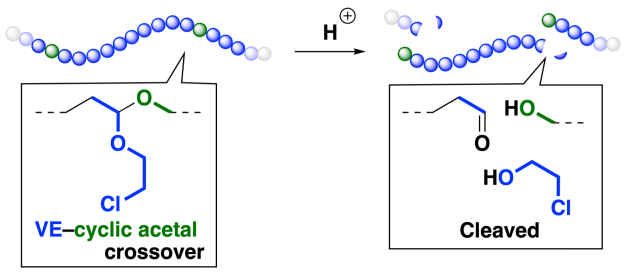

Scheme 2. Acid Hydrolysis of Copolymers via Cleavage of Acetal Moieties

Polymerization Mechanisms and Discussion on the Bulkiness of Sugar-Derived Cyclic Acetals

The reaction mechanisms of the crossover reactions of VE and E-1 are shown in Scheme 3A. E-1 adds to the propagating species derived from a VE to generate an oxonium ion. The oxonium ion undergoes ring-opening to generate a carbocation (oxocarbenium ion). This carbocation is stabilized by the electron-donating effects of a neighboring oxygen atom and methyl groups at the 2-position of E-1 (Scheme 3C). The carbocation stability is advantageous for efficient ring-opening reactions. The E-1-derived cation does not react with E-1 as confirmed by the nonhomopolymerizability of E-1 (Table S1), whereas it reacts with a VE. The E-1-derived carbocation potentially undergoes a ring-closing reaction to regenerate the oxonium ion (the reverse reaction of "Ring-opening" in Scheme 3) and subsequently the VE-derived cation and an E-1 monomer (the reverse reaction of "Crossover to E-1" in Scheme 3), while a reverse reaction does not occur once a VE reacts with the E-1-derived carbocation ("Crossover to VE" in Scheme 3) due to negligible cleavage of the carbon–carbon bond between E-1 and VE. The reverse reaction from the E-1-derived carbocation and the reaction of the E-1-derived carbocation and a VE likely correspond to thermodynamic and kinetic processes, respectively.

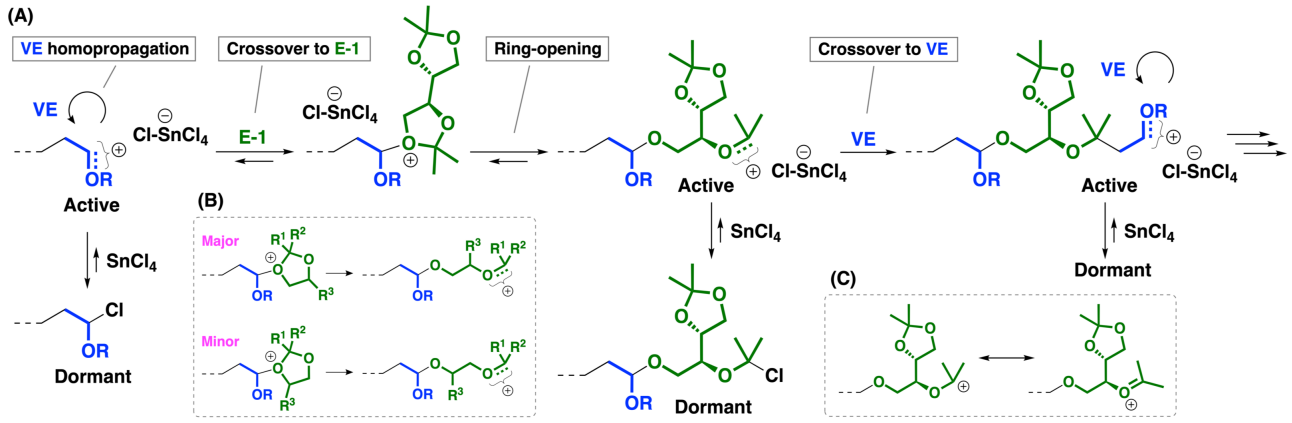

Scheme 3. (A) Copolymerization Mechanisms [A Lewis Base (Ethyl Acetate) Is Omitted]. (B) Ring-Opening Modes (Counteranions Are Omitted). (C) Resonance Structures of the E-1-Derived Cation.

The dormant–active equilibrium that consists of the reversible activation–deactivation of the carbon–chlorine bonds[46–53] is most likely constructed (Scheme 3A), which is responsible for the controlled/living copolymerization. The carbon–chlorine bond formed from the cyclic acetal-derived

carbocation (oxocarbenium ion) is reversibly cleavable under the conditions suited for VE polymerization due to the similarity between the carbocations generated from VEs and cyclic acetals. However, the E-1-derived carbocation has dimethyl groups, which is similar to the carbocation derived from α-methyl VEs.[54] This carbocation is more stable and more easily generated via the cleavage of the carbon–chlorine propagating ends than the CEVE-derived counterpart. Therefore, the CEVE-derived carbon–chlorine bonds are most likely dominant during polymerization. Such propagating ends are converted into the CEVE-derived ω-end acetals, which was detected by ^{1}H NMR (peaks 14 and 15 in Figure 3), by the reaction with a methanol quencher.[43] If the E-1-derived chain end reacts with the quencher, a ketal moiety is generated; however, such ketal structures are unstable and easily hydrolyzed into ketone structures as reported in our previous study on the living cationic polymerization of α-methyl VEs.[54]

The sugar-derived cyclic acetals used in this study have multiple cyclic acetal structures. However, only one of the cyclic acetal moieties in sugar-derived monomers reacted, while the other rings remained intact in the obtained copolymers in most cases. This is likely because the probability of the reaction with the cyclic acetal moieties in monomer molecules is much higher than that in polymer chains due to the low incorporated ratios of the cyclic acetals. Indeed, intermolecular reactions by the reaction of a propagating cation and the cyclic moieties in polymer chains occurred when a high incorporated ratio was achieved with X-4 as demonstrated below.

The ring-opening reaction of the asymmetric cyclic acetal moiety occurs in two possible manners via the reaction at either of the two oxygen atoms in a ring, resulting in different microstructures (Scheme 3B). The reaction of the cyclic acetal at the methylene-adjacent oxygen atom is likely preferential over that at the methine-adjacent oxygen atom due to the less steric hindrance around the former, as demonstrated in our previous study.[55]

M-4 and S-1 are diastereomers consisting of three five-membered cyclic acetal moieties, while the incorporated ratio of M-4 (4%) was higher than that of S-1 (2%) (the average number of CEVE/cyclic

acetal per block: 22/1.0 (M-4) and 51/1.0 (S-1) (entries 4 and 5 in Table 1; Figure S3). The difference in the steric configuration likely caused the difference in the copolymerization behavior. In addition, the average number of CEVE/E-1 or M-4 per block was estimated to be 18/1.0 or 22/1.0, respectively, via ^{1}H NMR analysis, indicating that the frequency of crossover reactions was similar between E-1 and M-4. Therefore, steric hindrance near the cyclic acetal moiety is likely more influential than that far from it. G-1, which has two five-membered cyclic acetal moieties and one cyclic hemiacetal ester moiety, was not incorporated into polymer chains. The reason why the copolymerization did not proceed with G-1, which has a structure similar to those of M-4 and S-1, is not clear.

From the reaction mechanism and the relationship between monomer structures and copolymerization behavior, we hypothesized that the bulkiness of the substituent on a cyclic acetal is largely responsible for the copolymerizability. To examine the effects of the substituent, the copolymerizations of CEVE and five-membered cyclic acetals having no (F-1), methyl (F-2), or propyl (F-3) group at the 4-position were conducted under the same conditions as those for the copolymerizations of CEVE and sugar-derived cyclic acetals (Table 2 and Figure S14). In all cases, the copolymerization proceeded via crossover reactions, which was confirmed by ^{1}H NMR (Figure S15). The average number of CEVE/ F-1, F-2, or F-3 per block was estimated to be 2.2/1.0, 5.1/1.0, or 8.7/1.0, respectively, via ^{1}H NMR analysis, which indicates that cyclic acetals with a bulkier substituent at the 4-position resulted in lower incorporation ratios in polymer chains. This trend is consistent with relatively low incorporated ratios of sugar-derived cyclic acetal monomers in the copolymerizations. In particular, the mannitol-derived monomers (M-1, M-2, and M-3) have substituents at all the four carbon atoms in the butylene unit of the seven-membered ring, which is obviously disadvantageous for copolymerization via ring-opening reactions compared to less bulky monomers such as the erythritol-derived monomers (Scheme 4; only the reaction at the seven-membered ring is shown because the carbocation generation is preferential due to the dimethyl groups). Indeed, in our previous study, a seven-membered cyclic acetal that does not have substituents in the butylene unit (2,2-dimethyl-1,3-dioxepane) underwent more

frequent crossover reactions in the copolymerization with VEs than the five-membered counterpart (2,2-dimethyl-1,3-dioxolane; F-1).[43] Therefore, the copolymerizability of cyclic acetals is most likely governed by several factors, such as ring-strain (six- < five- ~ seven-membered ring[43]), the stability of generated carbocations (affected by the substituents at the 2-position), and bulkiness around the diol-derived moiety.

Table 2. Cationic Copolymerization of F-1, F-2, or F-3 with CEVE [a]

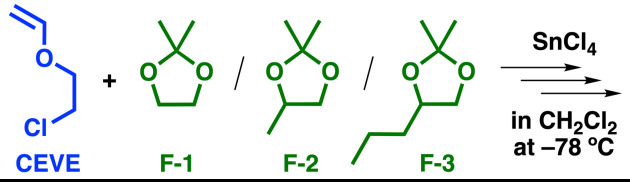

cyclic acetal	time (min)	conv (%)		$M_n \times 10^{-3}$ (calcd)[d]	$M_n \times 10^{-3}$ (exp)[e]	units per block[f]	
		CEVE [b]	cyclic acetal [c]			CEVE	cyclic acetal
F-1	3	>99	52	16.1	4.5	2.2	1.0
F-2	5	80	28	11.9	6.0	5.1	1.0
F-3	8	83	20	11.9	5.4	8.7	1.0

[a] $[CEVE]_0$ = 0.40 M, $[\text{cyclic acetal}]_0$ = 0.40 M, $[IBVE–HCl]_0$ = 4.0 mM, $[SnCl_4]_0$ = 20 mM, [ethyl acetate] = 50 mM, in dichloromethane at –78 ºC. [b] Determined by gas chromatography. [c] Determined by method A (see the experimental section for method A). [d] Calculated from the amounts of the cationogen and the consumed monomers: ($[CEVE]_0$ × conv × MW + $[\text{cyclic acetal}]_0$ × conv × MW)/$[IBVE–HCl]_0$. ($[CEVE]_0$ + $[\text{cyclic acetal}]_0$)/$[IBVE–HCl]_0$ = 200. [e] Determined by GPC (polystyrene standards). [f] Estimated by ^{1}H NMR analysis. After purification by preparative GPC. The ratios of monomer units in polymers are inconsistent with the values estimated by monomer conversion. Side products such as cyclic dimers are likely responsible for the inconsistency (Figure S15).

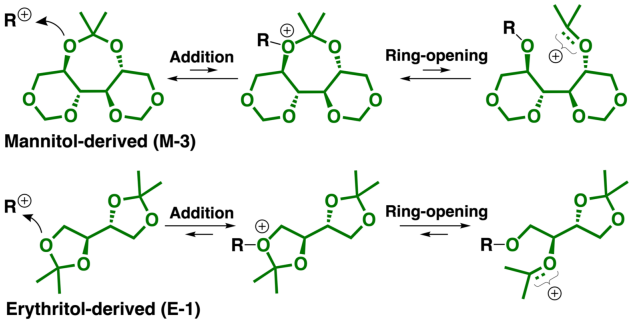

Scheme 4. Ring-Opening Reactions of M-3 and E-1

Bulkiness of the substituents at the carbon atom adjacent to two oxygen atoms did not affect the frequency of the crossover reactions. The average number of CEVE/E-2 (17/1.0) was comparable to that

of CEVE/E-1 (18/1.0) (entries 7 and 8 in Table 1) in the copolymers, which suggests the negligible difference between the cyclopentylidene group and the dimethyl groups.

Copolymerization of Xylose-Derived Monomers Bearing Aromatic Substituents

As demonstrated above (entries 11 and 12 in Table 1), the xylose-derived monomers bearing aromatic substituents (X-3 and X-4) were incorporated into polymer chains in the copolymerizations with CEVE despite the bulky structures (Figure 4). ^{1}H NMR analysis of the copolymer of CEVE and X-4 suggested that the crossover reactions occurred during copolymerization (Figure 5A). Xylose-derived monomer X-4 has five- and six-membered rings. When the six-membered ring opens, the five-membered ring remains in the side chain of the polymer (peak 10; 5.8–6.2 ppm[56]). On the other hand, when the five-membered ring opens, the six-membered ring remains in the side chain of the polymer (peak 21; 5.3–5.6 ppm[56]). ^{1}H NMR analysis indicates that both rings likely opened, whereas the six-membered ring more preferentially opened. In our previous study,[44] five- and six-membered cyclic acetals bearing a *p*-methoxyphenyl group at the 2-position exhibited comparable reactivity in the cationic copolymerization with VEs. A possible cause of the preferential ring-opening of the six-membered ring in X-4 is the electron-withdrawing effect of an oxygen atom adjacent to both C-1 and C-4 (Scheme 3). The electron-withdrawing effect is responsible for both lowered reaction frequency due to the decreased basicity of the other oxygen atom attached to C-1 and ineffective reactions at the C-2-adjacent oxygen atom due to the inefficient generation of an unstable carbocations that is adjacent to an acetal moiety.

The average number of CEVE/X-4 units per block was estimated to be 5.4/1.0, indicating that the frequency of crossover reactions was the highest among the sugar-derived cyclic acetals used in this study. Acid hydrolysis results (Figure 4B, purple; Figure 5B) also supported the copolymer structure resulting from frequent crossover reactions. The stabilization of a carbocation by the *p*-methoxyphenyl substituent is most likely responsible for the copolymerizability of X-4 (Scheme 5). The ring-opening is

likely facilitated by the stabilization of the structure after the oxonium ion opens. The stabilization by alkyl substituents is insufficient in the cases of X-1 and X-2, resulting in ineffective copolymerizations.[57]

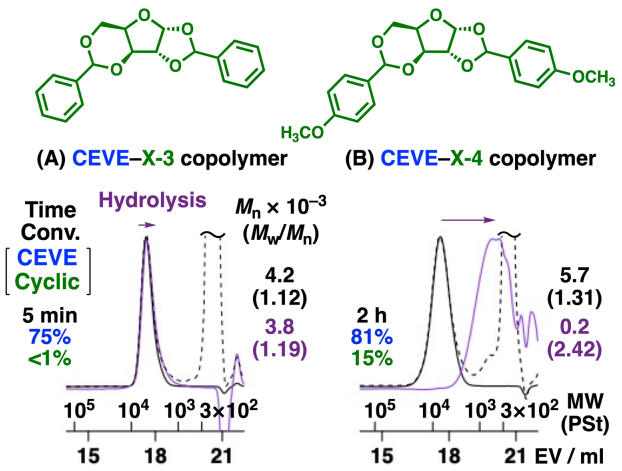

Figure 4. MWD curves of the (A) CEVE–X-3 (entry 11 in Table 1) and (B) CEVE–X-4 (entry 12) copolymers [black; before (dashed) and after (solid) purification by preparative GPC] and their hydrolysis products (purple; hydrolyzed after purification by preparative GPC). See Table 1 for the polymerization conditions.

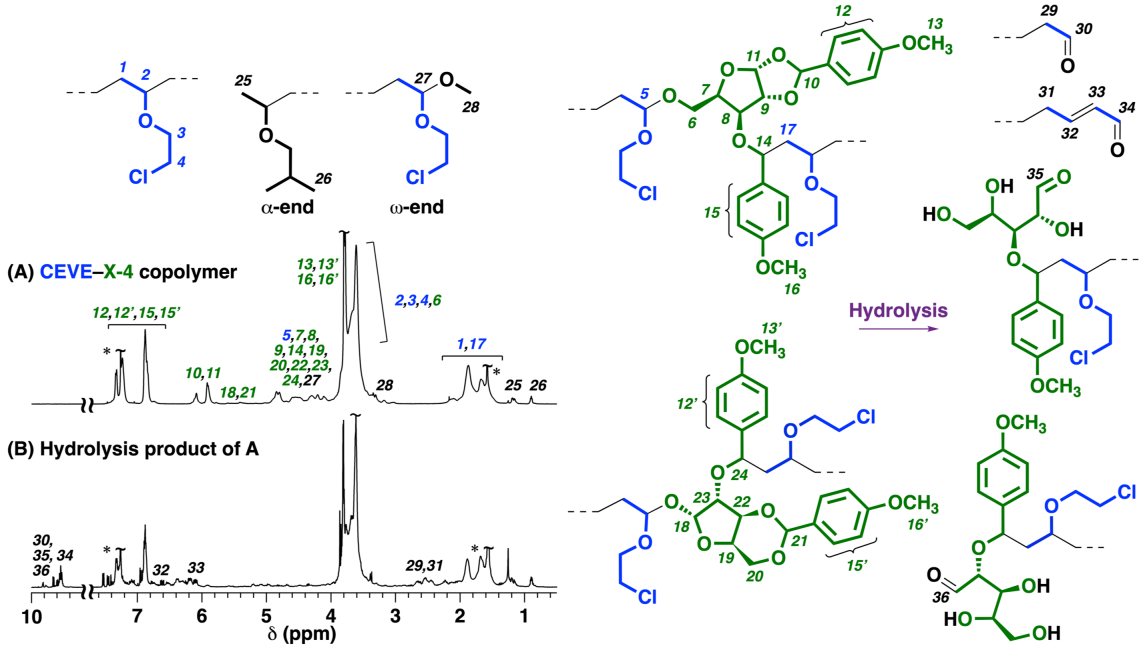

Figure 5. ^{1}H NMR spectra of (A) the CEVE–X-4 copolymer (entry 12 in Table 1; Figure 4B; after purification by preparative GPC) and (B) its hydrolysis product (purple curve in Figure 4B). * Water or $CHCl_3$.

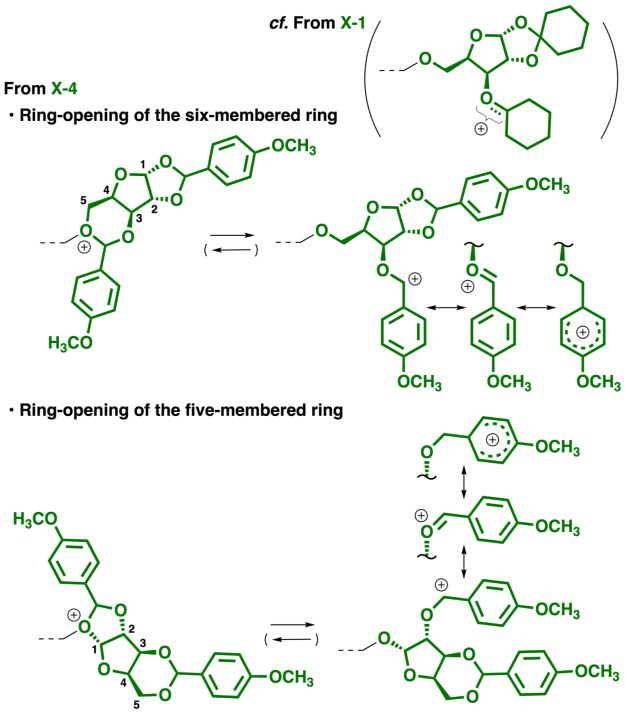

Scheme 5. Ring-Opening Modes of X-4.

The copolymerization of X-4 was also examined using IBVE or pMeSt (Scheme 1C) as comonomers (Table S3 and Figure S16). The average number of IBVE or pMeSt/X-4 per block was estimated to be 148/1.0 or 25/1.0, respectively, by ^{1}H NMR analysis (Figure S17). The results indicate that X-4 was incorporated into polymer chains, although the frequency of crossover reactions was much lower than the case with CEVE.

Effects of Initiators and Catalysts

To examine the effects of initiators and catalysts on the frequency of crossover reactions, we conducted copolymerizations of CEVE and E-1 using $GaCl_3$, Ph_3CPF_6, and $Ph_3CB(C_6F_5)_4$ instead of $SnCl_4$ (entries 1–4 in Table 3; Figure S18). The average number of CEVE/E-1 per block was 18/1.0 ($SnCl_4$), 15/1.0 ($GaCl_3$), 13/1.0 (Ph_3CPF_6), or 5.6/1.0($Ph_3CB(C_6F_5)_4$). The result suggests that the incorporation ratio of E-1 increased in the order of $SnCl_4$ < $GaCl_3$ < Ph_3CPF_6 < $Ph_3CB(C_6F_5)_4$. When $SnCl_4$, $GaCl_3$, Ph_3CPF_6, and $Ph_3CB(C_6F_5)_4$ are used, the counteranions that present near the propagating cations are $SnCl_5^-$, $GaCl_4^-$, PF_6^-, and $B(C_6F_5)_4^-$, respectively. The coordinating ability of the anions is likely related to this order, although there is no definitive scale of coordinating ability as far as we

know.[58–60] The weaker interaction between the propagating cation and the counteranion is most likely advantageous for easier access of the sugar-derived cyclic acetals to the propagating cation, resulting in more frequent crossover reactions when initiators or catalysts that generate counteranions with weaker coordinating ability were used. The influence of counteranions on crossover frequency was also observed in our recent study on cationic terpolymerization of VE, oxirane, and ketone;[61] however, a reason of such influences is unclear. From the results of the copolymerization of CEVE and E-1 using $Ph_3CB(C_6F_5)_4$, the monomer reactivity ratios of CEVE and E-1 were determined to be 5.0 (CEVE) and approximately 0 (E-1) (Figure S19 and Table S4; by the Meyer–Lowry method[62,63]), which were consistent with the nonhomopolymerizability of E-1. The values indicate that a copolymer obtained at equimolar amounts of CEVE and E-1 is expected to consist of CEVE blocks that have approximately six CEVE units in each block and E-1 blocks that have only one E-1 unit in each block. In addition, the proportion of E-1 in copolymers could be changed by the copolymerizations at different monomer concentrations (Figure S20 and Table S5). The CEVE/E-1 units per block were 19/1.0, 7.7/1.0, 5.3/1.0, 4.7/1.0, and 4.3/1.0 when copolymers were produced with $Ph_3CB(C_6F_5)_4$ at the CEVE/E-1 concentrations of 0.90 M/0.10 M, 0.70 M/0.30 M, 0.50 M/0.50 M, 0.40 M/0.60 M, and 0.30 M/0.70 M, respectively.

$Ph_3CB(C_6F_5)_4$ was effective for copolymerization of the cyclic acetals that did not undergo copolymerization with $SnCl_4$. When X-1 was copolymerized with CEVE by $Ph_3CB(C_6F_5)_4$, a very small amount of X-1 was incorporated into polymer chains (entry 6 in Table 3). In addition, the frequency of crossover reactions increased when X-3 was copolymerized by $Ph_3CB(C_6F_5)_4$ (entry 8 in Table 3) instead of $SnCl_4$.

Table 3. Cationic Copolymerizations of CEVE and E-1, X-1, X-3, or X-4 with Different Initiators or Catalysts [a]

entry	cyclic acetal	initiator or catalyst	time	conv (%)		$M_n \times 10^{-3}$ [d]	M_w/M_n [d]	units per block [e]	
				CEVE [b]	cyclic acetal [c]			CEVE	cyclic acetal
1	E-1	$SnCl_4$	8 min	81	5	8.1	1.08	18	1.0
2	E-1	$GaCl_3$	10 min	84	6	5.2	2.08	15	1.0
3	E-1	Ph_3CPF_6	45 min	92	7	37	2.01	13	1.0

4	E-1	$Ph_3CB(C_6F_5)_4$	75 min	75	13	21	2.32	5.6	1.0
5	X-1	$SnCl_4$	3 min	98	0	9.0	1.12	–	–
6	X-1	$Ph_3CB(C_6F_5)_4$	48 h	>99	<1	15	1.80	(192)	1.0
7	X-3	$SnCl_4$	5 min	75	<1	4.2	1.12	(165)	1.0
8	X-3	$Ph_3CB(C_6F_5)_4$	30 min	95	2	13	1.96	45	1.0
9	X-4	$SnCl_4$	2 h	81	15	5.7	1.31	5.4	1.0
10	X-4	$Ph_3CB(C_6F_5)_4$	2.8 h	89	34	19	5.66	2.6	1.0
11	X-4	$Ph_3CB(C_6F_5)_4$	17 h	>99	36	18[f]	12.7	2.7	1.0

[a] $[CEVE]_0$ = 0.40 M, $[cyclic\ acetal]_0$ = 0.40 M, $[IBVE–HCl]_0$ = 4.0 mM, $[SnCl_4]_0$ = 20 mM, [ethyl acetate] = 50 mM (entries 1,5,7, and 9); $[CEVE]_0$ = 0.50 M, $[cyclic\ acetal]_0$ = 0.50 M, $[IBVE–HCl]_0$ = 5.0 mM, $[GaCl_3]_0$ = 5.0 mM, [1,4-dioxane] = 0.30 M (entry 2); $[CEVE]_0$ = 0.50 M, $[cyclic\ acetal]_0$ = 0.50 M, $[initiator]_0$ = 1.0 mM (entries 3, 4, 6, 8, 10, and 11); in dichloromethane at –78 °C. Entries 1, 5, 7, and 9 correspond to entries 7, 9, 11, and 12 in Table 1, respectively. [b] Determined by gas chromatography. [c] Determined by methods B (except for entry 6) or C (entry 6) (see the experimental section for methods B and C). [d] Determined by GPC (polystyrene standards). [e] Estimated by ^1H NMR analysis. After purification by preparative GPC. [f] Insoluble parts were present. A portion of this sample exceeded the exclusion limit of the GPC column used.

The highest incorporated ratio was achieved when X-4 was copolymerized with $Ph_3CB(C_6F_5)_4$. The average number of CEVE/X-4 per block was 2.6/1.0 (entry 10 in Table 3; Figure 6A). Moreover, intermolecular reactions occurred between the propagating cation and the remaining cyclic acetal in polymer chains as confirmed by the appearance of a shoulder in the high-MW region in the MWD curve (entry 11; Figure 6B). The increased probability of the reactions of the propagating cation and the cyclic acetal moieties in polymer chains is responsible for this result as a result of increased amounts of the latter due to the high incorporated ratio of X-4.

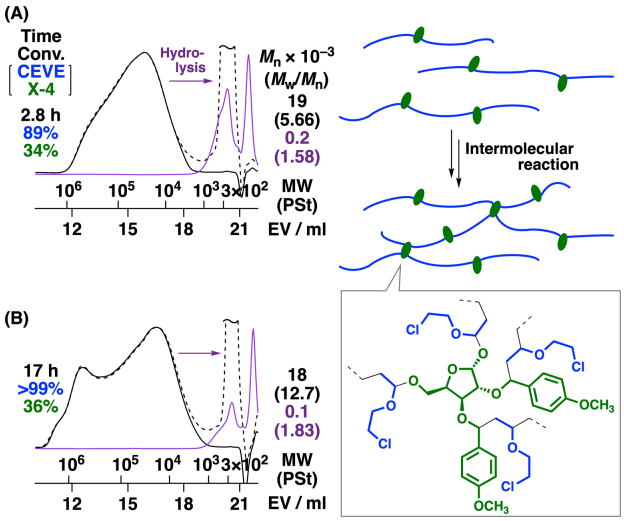

Figure 6. MWD curves of the CEVE–X-4 copolymers obtained by $Ph_3CB(C_6F_5)_4$ for (A) short (entry 10 in Table 3) or (B) long (entry 11) reaction time [black; before (dashed) and after (solid) purification by preparative GPC] and the hydrolysis product (purple; hydrolyzed after purification by preparative GPC). See Table 3 for the polymerization conditions.

Cationic Copolymerization of Oxiranes and Sugar-Derived Monomers Bearing Cyclic Hemiacetal Ester Moiety

Monomers with a cyclic hemiacetal ester structure potentially undergo copolymerization with oxiranes, as demonstrated in our previous study.[64] G-1 has a cyclic hemiacetal ester moiety; hence, cationic copolymerization of G-1 and VCHO (Scheme 1C) was conducted using $B(C_6F_5)_3$ as a catalyst in dichloromethane at −78 °C. The polymerization proceeded smoothly to yield a polymer with a unimodal MWD (entry 1 in Table 4; Figure 7).

Table 4. Cationic Copolymerization of G-1 or T-1 with an Oxirane [a]

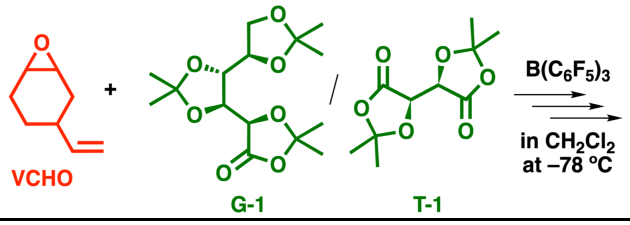

entry	monomer	time	conv (%)		$M_n \times 10^{-3}$ [d]	M_w/M_n [d]	units per block [e]	
			VCHO [b]	G-1 or T-1 [c]			VCHO	G-1 or T-1
1	G-1	10 s	93	23	5.0	1.67	5.6	1.0
2	T-1	10 s	>99	15	5.8	2.66	11	1.0

[a] $[VCHO]_0 = 0.50$ M, $[G\text{-}1 \text{ or } T\text{-}1]_0 = 0.50$ M, $[B(C_6F_5)_3]_0 = 3.0$ mM, in dichloromethane at −78 °C. [b] Determined by gas chromatography. [c] Determined by method C (see the experimental section for method C). [d] Determined by GPC (polystyrene standards). [e] Estimated by ^{1}H NMR analysis. After purification by preparative GPC.

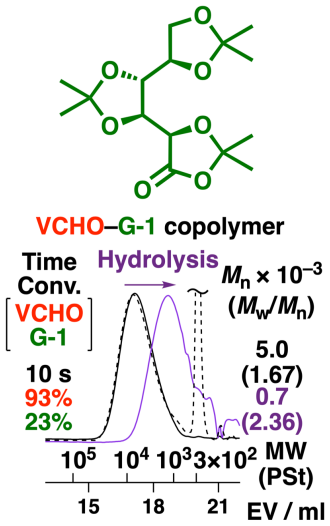

Figure 7. MWD curves of the VCHO–G-1 copolymer [entry 1 in Table 4; black; before (dashed) and after (solid) purification by preparative GPC] and the hydrolysis product (purple; hydrolyzed after purification by preparative GPC). See Table 4 for the polymerization conditions.

^{1}H NMR analysis of the copolymer of VCHO and G-1 (Figure 8A) exhibited both VCHO-derived peaks (peaks 1 and 4–7) and G-1-derived peaks (peaks 9–12 and 16). A peak of an ester-adjacent methine proton (peak 8), which was derived from the crossover reaction from VCHO to G-1, overlapped with other peaks (peaks 6 and 7), although the methine peak likely existed as judged from the integral ratios. The carbonyl group-adjacent methine proton of the monomer (peak a) was observed around 4.6 ppm (Figure 8B), while peaks were not detected in this region in the spectrum of the copolymer. The result suggests that not the cyclic acetal moiety but the cyclic hemiacetal ester moiety of G-1 reacted in the copolymerization. Specifically, an oxirane-derived oxonium ion reacts with the carbonyl group of G-1 to generate an ester moiety and a G-1-derived cation (Scheme S2). The G-1-derived cation reacts with VCHO to generate a ketal moiety in the main chain. The average number of VCHO/G-1 units per block was estimated to be 5.6/1.0 from the integral ratios (Figure 8A). In addition, the monomer reactivity ratios of VCHO and G-1 were determined to be 3.7 (VCHO) and approximately 0 (G-1) (Figure S21 and Table S6; by the Kelen–Tüdõs method),[65,66] which were consistent with the nonhomopolymerizability of G-1.

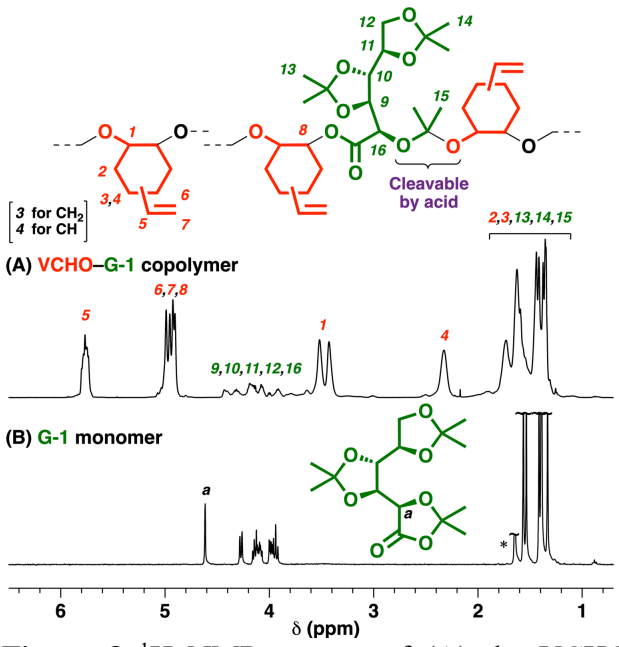

Figure 8. ^{1}H NMR spectra of (A) the VCHO–G-1 copolymer (entry 1 in Table 4; Figure 7; after purification by preparative GPC) and (B) G-1 monomer. * Water.

The VCHO–G-1 copolymer has ketal moieties in the main chain; hence, the copolymers could be hydrolyzed by acid. The hydrolysis product had a lower M_n value than the original copolymer (Figure 7, purple), which supports the occurrence of crossover reactions from G-1 to VCHO in the copolymerization.

T-1,[37,67] which is a cyclic hemiacetal ester derived from L-(+)-tartaric acid, was also copolymerized with VCHO (entry 2 in Table 4; Figure S22). The average number of VCHO/T-1 per block was 11/1.0, respectively (Figure S23), indicating that the frequency of crossover reactions was lower than that of G-1.

As in the case of our previous study on polymerizations of cyclic hemiacetal esters, G-1 and T-1 also underwent cationic terpolymerization with VE and oxiranes. For example, IPVE, VCHO, and G-1 were polymerized to yield a terpolymer with an M_n of 6.2 × 10^3 (Table S7). The number of IPVE/VCHO/G-1 units per block was 2.6/2.6/1.0. IPVE was likely incorporated into polymer chains as a result of the crossover reactions from the G-1-derived carbocation to IPVE (Scheme S3). The detailed results are shown in the Supporting Information (Table S7, Scheme S3, and Figures S24 and S25).

Summary of the Copolymerizations

The results of the copolymerizations conducted in this study are summarized in Chart 1. The polymerizability of cyclic acetals depends on several factors, such as ring-strain, the stability of generated carbocations, and bulkiness. The obtained results suggest that steric factors concerning bulkiness likely affected the polymerizability of the sugar-derived cyclic acetals more heavily than ring strain. M-1, M-2, M-3, X-1, and X-2, which have bulky structures, did not undergo copolymerization with CEVE. In contrast, the copolymerization proceeded when E-1, E-2, M-4, and S-1 were combined with CEVE. M-4, S-1, and G-1 have similar structures, while the copolymerizability differed depending on the configuration of the monomers and the presence of a cyclic hemiacetal ester moiety. Unlike X-1 and X-2, which have alkyl groups at the 2-potision of the cyclic acetal moieties, X-3 and X-4, which are the aryl group-containing counterparts, underwent cationic copolymerization with CEVE. In particular, X-4, which has *p*-methoxyphenyl groups, was the most effective for copolymerization among the sugar-derived cyclic acetals examined in this study.

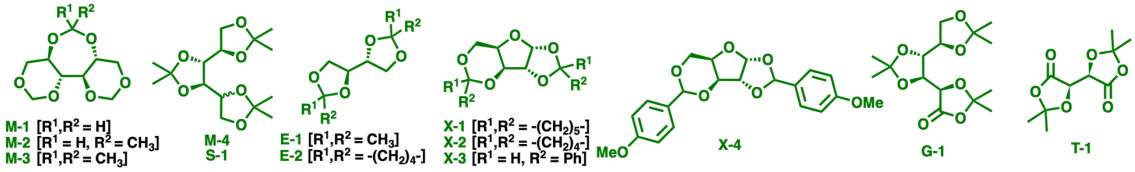

Structural features	Cyclic acetal	Cyclic acetal	Cyclic acetal	Cyclic acetal	Cyclic acetal	Cyclic acetal, Cyclic hemiacetal ester	Cyclic hemiacetal ester
Copolymerization with VE	VE homopolymer	Copolymer	Copolymer	VE homopolymer (X-1 and X-2) or slightly incorporated (X-3)	Copolymer (Most effective)	VE homopolymer in copolymn	–
						Terpolymer from VE and oxirane	Terpolymer from VE and oxirane
Copolymerization with Oxirane	–	–	–	–	–	Copolymer	Copolymer

Chart 1. Summary of the Copolymerizations Examined in This Study

G-1 did not undergo copolymerization with CEVE, while the copolymerization with an oxirane proceeded via the reaction of not the cyclic acetal but cyclic hemiacetal ester moiety. T-1, which is derived from tartaric acid, was also copolymerized with an oxirane via reaction of the cyclic hemiacetal ester moiety.

Thermal Properties of Copolymers

The thermal properties of the copolymers were examined by differential scanning calorimetry (DSC) and thermogravimetric analysis (TGA) (Figures S26 and S27). The CEVE–E-1 copolymers and the CEVE homopolymer exhibited comparable glass transition temperatures (T_gs) (–26 and –33 ºC; entries 1, 2, and 5 in Table 5), while the CEVE–X-4 copolymers exhibited considerably higher T_gs (28 and 33 ºC; entries 3 and 4). The aryl substituents and/or the fused ring structures of X-4 units in copolymer chains are likely responsible for the higher T_gs of the CEVE–X-4 copolymers than those of the CEVE–E-1 copolymers and the CEVE homopolymer. The VCHO–G-1 copolymer exhibited a lower T_g (2 ºC; entry 6) than that of a VCHO homopolymer (50 ºC;[68] entry 7). In TGA analysis, the copolymers began to degrade at around 200 °C (Figure S27). Temperatures corresponding to 5% (T_{d5}) and 20% (T_{d20}) weight loss are listed in Table 5.

Table 5. T_g, T_{d5}, and T_{d20} Values of the Obtained Polymers[a]

entry	polymer	units per block [b]		$M_n \times 10^{-3}$ [c]	M_w/M_n [c]	T_g (ºC)[d]	T_{d5} (ºC)[e]	T_{d20} (ºC)[e]
		CEVE or VCHO	sugar-derived monomer					
1	CEVE–E-1 copolymer	16	1.0	6.7	1.16	–26	186	252
2	CEVE–E-1 copolymer	4.3	1.0	8.4	2.05	–26	–	–
3	CEVE–X-4 copolymer	5.4	1.0	6.4	1.21	28	216	246
4	CEVE–X-4 copolymer	2.6	1.0	24	4.34	33	–	–
5	CEVE homopolymer	–	–	6.5	1.10	–33	104	269
6	VCHO–G-1 copolymer	5.6	1.0	4.5	1.70	2	241	327
7	VCHO homopolymer	–	–	45	1.95	50	368	409

[a] After purification by preparative GPC. Entry 1: obtained under the same conditions as those for entry 7 in Table 1. Entry 2: obtained under the same conditions as those for entry 5 in Table S5. Entry 3: entry 12 in Table 1. Entry 4: entry 10 in Table 3. Entry 5: $[CEVE]_0 = 0.40$ M, $[IBVE–HCl]_0 = 4.0$ mM, $[SnCl_4]_0 = 20$ mM, [ethyl acetate] = 50, mM, in dichloromethane at –78 ºC. Entry 6: entry 1 in Table 4. Entry 7: $[VCHO]_0 = 0.26$ M, $[B(C_6F_5)_3]_0 = 1.0$ mM, in dichloromethane at −78 °C (reference 68). [b] Calculated by ^{1}H NMR. [c] Determined by GPC (polystyrene calibration). [d] By DSC (second heating scan, at 10 °C min^{-1}; see Figure S26). [e] By TGA (see Figure S27).

Conclusion

Sugar-derived cyclic acetals with appropriate structures underwent cationic copolymerization with CEVE. Specifically, structural features, such as the number of cyclic acetal moieties, the number of ring members, substituents, and stereo configuration, were highly responsible for copolymerization behavior. Mannitol-derived cyclic acetals with three fused rings were inert for copolymerization. Erythritol-derived cyclic acetals with two five-membered rings underwent copolymerization with CEVE in a living manner under appropriate conditions. Mannitol- or sorbitol-derived cyclic acetals with three five-membered rings exhibited different reactivities likely due to the difference in stereo configuration. The xylose-derived cyclic acetal that has a *p*-methoxyphenyl substituent at the carbon atom adjacent to two oxygen atoms underwent copolymerization with CEVE very effectively, while other xylose-derive cyclic acetals, which have alkyl or phenyl substituents, exhibited very low reactivity. In addition, cationic initiators and Lewis acid catalysts affected the incorporated ratios of cyclic acetals. A cationic initiator that generates a non-coordinating counteranion was effective for copolymerization via frequent crossover reactions. A gluconic acid-derived cyclic acetal that has both cyclic acetal and cyclic hemiacetal ester moieties was not incorporated into polymer chains by the copolymerization with CEVE, while copolymers were obtained via the ring-opening of the cyclic hemiacetal ester moiety when oxiranes were used as comonomers. The results obtained in this study contribute to the developments of sugar-derived polymer synthesis by cationic copolymerization.

Associated Content

Supporting Information
Experimental section, polymerization data, and NMR spectra of polymers.

Corresponding Author
E-mail: kanazawaa11@chem.sci.osaka-u.ac.jp

Notes
The authors declare no competing financial interest.

Acknowledgments

This work was partially supported by JSPS KAKENHI Grant 23H02010.

References and Notes

1. Ikada, Y.; Tsuji, H. Biodegradable Polyesters for Medical and Ecological Applications. *Macromol. Rapid Commun.* **2000**, *21*, 117–132.
2. Kimura, Y. Molecular, Structural, and Material Design of Bio-Based Polymer. *Polym. J.* **2009**, *41*, 797−807.
3. Farah, S.; Anderson, D. G.; Langer, R. Physical and Mechanical Properties of PLA, and Their Functions in Widespread Applications—A Comprehensive Review. *Adv. Drug Deliv. Rev.* **2016**, *107*, 367–392.
4. Galbis, J. A.; de Gracia Garcia-Martin, M.; Violante de Paz, M.; Galbis, E. Synthetic Polymers from Sugar-Based Monomers. *Chem. Rev.* **2016**, *116*, 1600–1636.
5. Santoro, O.; Izzo, L.; Della Monica, F. Recent Advances in RO(CO)P of Bio-Based Monomers. *Sustain. Chem.* **2022**, *3*, 259–285.
6. Wang, J.; Zhou, J.; Ding, Y.; Hu, X.; Chen, Y. Glycopolymers Based on Carbohydrate or Vinyl Backbones and Their Biomedical Applications. *Polym. Chem.* **2023**, *14*, 2414–2434.
7. Uryu, T.; Koyama, Y.; Matsuzaki, K. Cationic Ring-Opening Polymerization of 3,5-Anhydro-1,2-*O*-isopropylidene-α-D-xylofuranose. *J. Polym. Sci., Polym. Lett. Ed.* **1979**, *17*, 673–678.
8. Uryu, T.; Koyama, Y.; Matsuzaki, K. Selective Ring-Opening Polymerization of 3,5-Anhydro-1,2-*O*-isopropylidene-α-D-xylofuranose Synthesis of [3→5]-D-xylan. *Makromol. Chem.* **1984**, *185*, 2099–2107.
9. McGuire, T. M.; Bowles, J.; Deane, E.; Farrar, E. H. E.; Grayson, M. N.; Buchard, A. Control of Crystallinity and Stereocomplexation of Synthetic Carbohydrate Polymers from D- and L-Xylose. *Angew. Chem. Int. Ed.* **2021**, *60*, 4524–4528.
10. McGuire, T. M.; Clark, E. F.; Buchard, A. Polymers from Sugars and Cyclic Anhydrides: Ring-Opening Copolymerization of a D-Xylose Anhydrosugar Oxetane. *Macromolecules* **2021**, *54*, 5094–5105.
11. Clark, E. F.; Kociok-Köhn G.; Davidson, M. G. Buchard, A. Polymers from Sugars and Isothiocyanates: Ring-Opening Copolymerization of D-Xylose Anhydrosugar Oxetane. *Polym. Chem.* **2023**, *14*, 2838–2847.
12. McGuire, T. M.; Buchard, A. Polymers from Sugars and CS_2: Ring Opening Copolymerization of a D-Xylose Anhydrosugar Oxetane. *Polym. Chem.* **2021**, *12*, 4253–4261.
13. Tran, D. K.; Rashad, A. Z.; Darensbourg, D. J.; Wooley, K. L. Sustainable Synthesis of CO_2-derived Polycarbonates from D-xylose. *Polym. Chem.* **2021**, *12*, 5271–5278.
14. Strietholt, W. A.; Thiem, J.; Höweler, U. F. B. Synthesis and Ring-Opening Polymerization of 1,4:2,5:3,6-Trianhydro-D-mannitol and Structure Studies by MNDO Calculations. *Makromol. Chem.* **1991**, *192*, 317–331.
15. Saxon, D. J.; Nasiri, M.; Mandal, M.; Maduskar, S.; Dauenhauer, P. J.; Cramer, C. J.; LaPointe, A. M.; Reineke, T. M. Architectural Control of Isosorbide-Based Polyethers via Ring-Opening Polymerization. *J. Am. Chem. Soc.* **2019**, *141*, 5107–5111.
16. Okada, M. Ring-Opening Polymerization of Heterobicyclic Compounds. Syntheses of Specialty Polymers. *Prog. Polym. Sci.* **1991**, *16*, 1027–1074.
17. Uryu, T. Artificial Polysaccharides and Their Biological Activities. *Prog. Polym. Sci.* **1993**, *18*, 717–761.
18. Yoshida, T. Synthesis of Polysaccharides Having Specific Biological Activities. *Prog. Polym. Sci.* **2001**, *26*, 379–441.
19. Kubisa, P.; Vairon, J. P. In *Polymer Science: A Comprehensive Reference*; Matyjaszewski, K., Möller, M., Eds.; Elsevier B.V.: Amsterdam, 2012; Vol. *4.10*.
20. Shen, T.; Chen, K.; Chen, Y.; Ling, J. Ring-Opening Polymerization of Cyclic Acetals: Strategy for Both Recyclable and Degradable Materials. *Macromol. Rapid Commun.* **2023**, *44*, 2300099.

21. Debsharma, T.; Yagci, Y.; Schlaad, H. Cellulose-Derived Functional Polyacetal by Cationic Ring-Opening Polymerization of Levoglucosenyl Methyl Ether. *Angew. Chem. Int. Ed.* **2019**, *51*, 18492–18495.
22. Wu, L.; Zhou, Z.; Sathe, D.; Zhou, J.; Dym, S.; Zhao, Z. Wang, J.; Niu, J. Precision Native Polysaccharides from Living Polymerization of Anhydrosugars. *Nat. Chem.* **2023**, *15*, 1276–1284.
23. Mizukami, Y.; Kakehi, Y.; Li, F.; Yamamoto, T.; Tajima, K.; Isono, T.; Satoh, T. Chemically Recyclable Unnatural (1→6)-Polysaccharides from Cellulose-Derived Levoglucosenone and Dihydrolevoglucosenone. *ACS Macro Lett.* **2024**, *13*, 252–259.
24. Haskins, W. T.; Hann, R. M.; Hudson, C. S. 2,3,4,5-Dimethylene-D-mannitol and a Second Dimethylene-D-mannitol. *J. Am. Chem. Sci.* **1943**, *65*, 67–70.
25. Ness, A. T.; Hann, R. M.; Hudson, C. S. The Acetolysis of Trimethylene-D-mannitol. 2,5-Methylene-D-mannitol. *J. Am. Chem. Soc.* **1943**, *65*, 2215–2222.
26. Grindley, T. B.; Stoddart, J. F.; Szarek, W. A. Conformational Studies on 1,3-Dioxepans. Part I. 1,3:2,5:4,6-Tri-*O*-methylene-D-mannitol and Some Related Compounds. *J. Chem. Soc. B* **1969**, 172–175.
27. Grindley, T. B.; Stoddart, J. F.; Szarek, W. A. Conformational Studies on 1,3-Dioxepans. Part II. 1,3:2,5:4,6-Tri-*O*-ethylidene-D-mannitol and Some Related Compounds. *J. Chem. Soc. B* **1969**, 623–626.
28. Heyns, K.; Lenz, J. Über Katalytische Oxydationen, XVI: Über die Darstellung von Penturonsäuren. *Chem. Ber.* **1961**, *94*, 348–352.
29. Tronchet, J. M. J.; Zosimo-Landolfo, G.; Villedon-Denaide, F.; Balkadjian, M.; Cabrini, D.; Barbalat-Rey, F. Synthetic Usefulness of the Sugar Cyclopentylidene Ketals. *J. Carbohydr. Chem.* **1990**, *9*, 823–835.
30. Ferrier, R. J.; Hatton, L. R. The Acid-Catalysed Condensation of D-Xylose with Benzaldehyde in the Presence of Alcohols. Two Diastereoisomeric 1,2:3,5-Di-*O*-benzylidene-α-D-xylofuranose. *Carbohydr. Res.* **1967**, *5*, 132–139.
31. Speier, A. Ueber die Verbindungen des Acetons mit Einigen Mehrwerthigen Alkoholen. *Ber. Dtsch. Chem. Ges.* **1895**, *28*, 2531–2534.
32. El Ashry, E. S. H. Recognition of the *threo* and *erythro* Isomers of 1-C-Substituted Glycerols. *J. Chem. Soc., Chem. Commun.* **1986**, 1024–1026.
33. Awal, A.; Boyd, A. S. F.; Buchanan, J. G.; Edgar, A. R. The Formation of Isopropylidene Acetals of Erythritol and Ribitol under Conditions of Kinetic Control. *Carbohydr. Res.* **1990**, *205*, 173–179.
34. Micovic, V. M.; Stojilikovic, A. The Condensations of Polyhydric Alcohols and Monosaccharides with Cyclopentanone and Cyclohexanone. *Tetrahedron* **1958**, *4*, 186–196.
35. Haworth, W. N.; Hirst, E. L.; Chamberlain, K. A. Acetone Derivatives of Gluconic Acid. *J. Chem. Soc.* **1937**, 795–797.
36. Jarosz, S.; Zamqjski, A. A Facile Synthesis of 1,2:3,4:5,6-Tri-*O*-isopropylidene-D-gluconate–A Convenient Precursor of the Open Chain Form of D-Glucose. *J. Carbohydr. Chem.* **1993**, *12*, 1223–1228.
37. Fischer, H. O. L.; Taube, C. Über Acetonieren mit Aceton und Zinkchlorid. *Ber. Dtsch. Chem. Ges.* **1927**, *60*, 485–490.
38. Sartori, S. K.; Miranda, I. L.; de Matos, D. A.; Kohlhoff, M.; Diaz, M. A. N.; Diaz-Munoz, G. Synthetic Studies toward (–)-Cleistenolide: Highly Stereoselective Synthesis of New γ-Lactone Subunits. *J. Braz. Chem. Soc.* **2021**, *32*, 757–766.
39. Onorato, A.; Pavlik, C.; Invernale, M. A.; Berghorn, I. D.; Sotzing, G. A.; Morton, M. D.; Smith, M. B. Polymer-Mediate Cyclodehydration of Alditols and Ketohexoses. *Carbohydr. Res.* **2011**, *346*, 1662–1670.
40. Okada, M.; Yamashita, Y.; Ishii, Y. Cationic Copolymerization of 1,3-Dioxolane with Styrene. *Makromol. Chem.* **1966**, *94*, 181–193.

41. Okada, M.; Yamashita, Y. Cationic Copolymerization of Cyclic Formals and Vinyl Ethers. *Makromol. Chem.* **1969**, *126*, 266−275.
42. Shirouchi, T.; Kanazawa, A.; Aoshima, S. Controlled Cationic Copolymerization of Vinyl Monomers and Cyclic Acetals via Concurrent Vinyl-Addition and Ring-Opening Mechanisms. *Macromolecules* **2016**, *49*, 7184–7195.
43. Maruyama, K.; Kanazawa, A.; Aoshima, S. Controlled Cationic Copolymerization of Vinyl Monomers and Cyclic Acetals *via* Concurrent Vinyl-Addition and Ring-Opening Mechanisms: The Systematic Study of Structural Effects on the Copolymerization Behavior. *Polym. Chem.* **2019**, *10*, 5304–5314.
44. Maruyama, K.; Kanazawa, A.; Aoshima, S. Alternating Cationic Copolymerization of Vinyl Ethers and Aryl-Substituted Cyclic Acetals: Structural Investigation of Effects of Cyclic Acetals on Copolymerizability. *Macromolecules* **2022**, *55*, 4034–4045.
45. E-3 (Scheme S1), which has a structure similar to that of E-2, was hardly soluble in dichloromethane at –78 ºC.
46. Sawamoto, M. Modern Cationic Vinyl Polymerization. *Prog. Polym. Sci.* **1991**, *16*, 111–172.
47. Kennedy, J. P.; Iván, B. *Designed Polymers by Carbocationic Macromolecular Engineering: Theory and Practice*; Hanser: New York, 1992.
48. Matyjaszewski, K.; Sawamoto, M. In *Cationic Polymerizations*; Matyjaszewski, K., Ed.; Marcel Dekker: New York, 1996; Chapter 4.
49. Kennedy, J. P. Living Cationic Polymerization of Olefins. How Did the Discovery Come About? *J. Polym. Sci., Part A: Polym. Chem.* **1999**, *37*, 2285–2293.
50. Puskas, J. E.; Kaszas, G. Living Carbocationic Polymerization of Resonance-Stabilized Monomers. *Prog. Polym. Sci.* **2000**, *25*, 403–452.
51. De, P.; Faust, R. In *Macromolecular Engineering. Precise Synthesis, Materials Properties, Applications*; Matyjaszewski, K., Gnanou, Y., Leibler, L., Eds.; Wiley-VCH GmbH & Co. KGaA: Weinheim, 2007; Chapter 3.
52. Goethals, E. J.; Du Prez, F. Carbocationic Polymerizations. *Prog. Polym. Sci.* **2007**, *32*, 220–246.
53. Aoshima, S.; Kanaoka, S. A Renaissance in Living Cationic Polymerization. *Chem. Rev.* **2009**, *109*, 5245–5287.
54. Yonezumi, M.; Takaku, R.; Kanaoka, S.; Aoshima, S. Living Cationic Polymerization of α-Methyl Vinyl Ethers Using $SnCl_4$. *J. Polym. Sci., Part A: Polym. Chem.* **2008**, *46*, 2202–2211.
55. Maruyama, K.; Kanazawa, A.; Aoshima, S. ABC-Type Periodic Terpolymer Synthesis by a One-Pot Approach Consisting of Oxirane- and Carbonyl-Derived Cyclic Acetal Generation and Subsequent Living Cationic Alternating Copolymerization with a Vinyl Monomer. *Macromolecules* **2022**, *55*, 799–809.
56. Sittiwong, W.; Richardson, M. W.; Schiaffo, C. E.; Fisher; T. J.; Dussault, P. H. Re_2O_7-Catalyzed Reaction of Hemiacetals and Aldehydes with *O*-, *S*-, and *C*-Nucleophiles. *Beilstein J. Org. Chem.* **2013**, *9*, 1526-1532.
57. To synthesize copolymers via frequent crossover reactions, we attempted to introduce an aryl group into the erythritol-derived monomer. However, phenyl or *p*-octyloxyphenyl group-containing monomers were hardly soluble in dichloromethane and thus copolymerization could not be conducted (Scheme S1).
58. The coordinating ability is probably in the order of $SnCl_5^-$ < PF_6^- < $B(C_6F_5)_4^-$ as judged from some studies (e.g. references 59 and 60) and the cationic polymerizations using $SnCl_4$ as a Lewis acid catalyst (references 46–53). It is unclear where $GaCl_4^-$ is placed in this order.
59. Castellanos, F.; Fouassier, J. P.; Priou, C.; Cavezzan, J. Synthesis, Reactivity, and Properties of New Diaryliodonium Salts as Photoinitiators for the Cationic Polymerization of Epoxy Silicones. *J. Appl. Polym. Sci.* **1996**, *60*, 705–713.
60. Aldrich, K. E.; Billow, B. S.; Holmes, D.; Bemowski, R. D.; Odom, A. L. Weakly Coordinating Yet Ion Paired: Anion Effects on an Internal Rearrangement. *Organometallics* **2017**, *36*, 1227–1237.

61. Eguchi, Y.; Kanazawa, A.; Aoshima, S. Metal-Free, Photoinitiated Cationic Terpolymerization of Vinyl Ethers, Oxiranes, and Ketones: Simultaneous Control of Monomer Sequence and Molecular Weight by the Formation of Long-Lived Propagating Species. *Macromolecules* **2024**, *57*, 3346–3357.
62. Meyer, V. E.; Lowry, G. G. Integral and Differential Binary Copolymerization Equations. *J. Polym. Sci. Part A* **1965**, *3*, 2843–2851.
63. Lynd, N. A.; Ferrier, Jr., R. C.; Beckingham, B. S. Recommendation for Accurate Experimental Determination of Reactivity Ratios in Chain Copolymerization. *Macromolecules* **2019**, *52*, 2277–2285.
64. Hyoi, K.; Kanazawa, A.; Aoshima, S. Cationic Ring-Opening Co- and Terpolymerizations of Lactic Acid-Derived 1,3-Dioxolan-4-ones with Oxiranes and Vinyl Ethers: Nonhomopolymerizable Monomer for Degradable Co- and Terpolymers. *ACS Macro Lett.* **2019**, *8*, 128–133.
65. Kelen, T.; Tüdõs, F. A New Improved Linear Graphical Method for Determining Copolymerization Reactivity Ratios. *React. Kinet. Catal. Lett.* **1974**, *1*, 487–492.
66. Kennedy, J. P.; Kelen, T.; Tüdõs, F. Analysis of the Linear Methods for Determining Copolymerization Reactivity Ratios. II. A Critical Reexamination of Cationic Monomer Reactivity Ratios. *J. Polym. Sci., Polym. Chem. Ed.* **1975**, *13*, 2277–2289.
67. De Giglio, E.; Bonifacio, M. A.; Cometa, S.; Vona, D.; Mattioli-Belmonte, M.; Dicarlo, M.; Ceci, E.; Fino, V.; Cicco, S. R.; Farinola, G. M. Exploiting a New Glycerol-Based Copolymer as a Route to Wound Healing: Synthesis, Characterization and Biocompatibility Assessment. *Colloids Surf. B: Biointerfaces* **2015**, *136*, 600–611.
68. Takahashi, Y.; Kanazawa, A.; Aoshima, S. 3-Alkoxyphthalides as Nonhomopolymerizable, Highly Reactive Comonomers for ABC Pseudo-Periodic Terpolymers and Degradable Polymers via Cationic Co- and Terpolymerizations with Oxiranes and/or Vinyl Ethers. *Macromolecules* **2023**, *56*, 4198–4207.